Developmental Cell *10*, 601–613, May, 2006 ©2006 Elsevier Inc. DOI 10.1016/j.devcel.2006.02.021

Drosophila Decapping Protein 1, dDcp1, Is a Component of the *oskar* mRNP Complex and Directs Its Posterior Localization in the Oocyte

Ming-Der Lin,[1] Shih-Jung Fan,[1] Wei-Shan Hsu,[1] and Tze-Bin Chou[1,2,*]
[1] Institute of Molecular and Cellular Biology
College of Life Science
National Taiwan University
Number 1, Section 4
Roosevelt Road
Taipei, 10617
Taiwan

Summary

In *Drosophila*, posterior deposition of *oskar* (*osk*) mRNA in oocytes is critical for both pole cell and abdomen formation. Exon junction complex components, translational regulation factors, and other proteins form an RNP complex that is essential for directing *osk* mRNA to the posterior of the oocyte. Until now, it has not been clear whether the mRNA degradation machinery is involved in regulating *osk* mRNA deposition. Here we show that *Drosophila* decapping protein 1, dDcp1, is a posterior group gene required for the transport of *osk* mRNA. In oocytes, dDcp1 is localized posteriorly in an *osk* mRNA position- and dosage-dependent manner. In nurse cells, dDcp1 colocalizes with dDcp2 and Me31B in discrete foci that may be related to processing bodies (P bodies), which are sites of active mRNA degradation. Thus, as well as being a general factor required for mRNA decay, dDcp1 is an essential component of the *osk* mRNP localization complex.

Introduction

During *Drosophila* oogenesis, Osk is localized to the posterior end of the oocyte, where it nucleates polar granules and is both necessary and sufficient for abdomen and pole cell formation (Ephrussi et al., 1991; Kim-Ha et al., 1991; Ephrussi and Lehmann, 1992). *osk* mRNA is synthesized in nurse cells, forming a translationally repressed mRNP complex, and is transported to the oocyte (reviewed in Wilhelm and Smibert, 2005). Once in the oocyte, an intact microtubule network, as well as Staufen (Stau) and Kinesin heavy chain (Khc) motor protein, guides *osk* mRNA to the posterior end (St Johnston et al., 1991; Clark et al., 1994; Brendza et al., 2000).

The posterior localization of *osk* is mediated by various components, including the splicing and translational machinery. Exon junction complex components, such as Mago-nashi and *Drosophila* Y14/Tsunagi, interact with eIF4AIII and Barentsz (Btz), and are required for *osk* localization (Newmark and Boswell, 1994; van Eeden et al., 2001; Hachet and Ephrussi, 2001; Mohr et al., 2001; Palacios et al., 2004). Cup, a *Drosophila* eIF4E binding protein that colocalizes with both Btz and Ypsilon Schachtel (Yps), is a repressor of *osk* mRNA translation via its interaction with the translational repressor Bruno and regulates *osk* localization (Wilhelm et al., 2003; Nakamura et al., 2004). In addition, Exuperantia (Exu) can directly interact with Yps and forms an mRNP complex containing *osk* (Wilhelm et al., 2000). Yps is a Y box protein that antagonizes the stimulation of translation of *osk* mRNA by Oo18 RNA binding (Orb) (Mansfield et al., 2002). Orb mediates the cytoplasmic polyadenylation of *osk* mRNA (Chang et al., 1999; Castagnetti and Ephrussi, 2003) and interacts with Exu and Yps in an RNA-dependent manner (Mansfield et al., 2002). Although the role of Exu in *osk* mRNA localization is not yet fully understood, its interaction with Yps and Orb implies a fine integration between transportation and translational regulation.

There is currently little evidence for the involvement of the mRNA degradation machinery in the posterior localization of *osk*. *Saccharomyces cerevisiae* Dhh1p, whose *Drosophila* homolog Me31B is a component of the *osk* mRNP complex, is an activator of decapping and physically interacts with Dcp1p (Coller et al., 2001). In addition, mammalian Staufen 1 interacts with the nonsense-mediated decay factor Upf1 and directs the decay of ADP-ribosylation factor 1 mRNA in a novel mRNA decay pathway (Kim et al., 2005). Given that *Drosophila* Stau is required for the posterior transport of *osk* mRNA, it is possible that components of the mRNA degradation machinery can participate in the *osk* mRNP complex.

Eukaryotic polyadenylated mRNA can be degraded primarily by removal of the 3′ poly(A) tail, followed either by decapping and 5′ to 3′ exonucleolytic digestion, or by 3′ to 5′ exosome degradation (reviewed in Parker and Song, 2004). The cleavage of the 5′ cap structure represents a critical step in mRNA degradation and turnover. The two conserved eukaryotic decapping proteins, Dcp1 and Dcp2, function together as a holoenzyme. Dcp2 has been found to be the catalytic subunit but it is unclear whether Dcp1 also has intrinsic catalytic activity. The current model is that Dcp1 enhances the decapping activity of Dcp2, but by a currently unresolved mechanism (Beelman et al., 1996; Van Dijk et al., 2002; Lykke-Andersen, 2002; Wang et al., 2002; Steiger et al., 2003). In the cytosol, Dcp1 localizes in distinct foci with other proteins involved in 5′ to 3′ mRNA decay, including Dcp2, Dhh1, Edc3, the Lsm1-7 complex, and the 5′ to 3′ exonuclease Xrn1 (reviewed in Fillman and Lykke-Andersen, 2005). These foci are referred to as processing bodies (P bodies), which are sites of active mRNA degradation in yeast and mammalian cells (Sheth and Parker, 2003; Cougot et al., 2004).

RNAi studies indicate that dDcp1 is involved in the miRNA degradation pathway but not in nonsense-mediated mRNA decay in S2 cells (Gatfield and Izaurralde, 2004; Rehwinkel et al., 2005). However, not much more is known about the cytoplasmic localization of dDcp1 and/or its potential role(s) during development. Here, we characterize a *Drosophila Dcp1* mutation and

*Correspondence: tbchou@ntu.edu.tw
[2] Lab address: http://cell.lifescience.ntu.edu.tw/english/.%5Cfaculty_en%5Cchou_tb_en.htm

describe the dDcp1 protein distribution pattern. We show that dDcp1 is required for the proper degradation of *osk*, *bcd*, and *twe* in the embryo and, as a component of the *osk* mRNP complex, that it is specifically required for the posterior localization of *osk* mRNA in the oocyte. In nurse cell cytoplasm, dDcp1 colocalizes with dDcp2 (*Drosophila* decapping protein 2) and Me31B in discrete foci. Also, dDcp1 is required for the proper posterior localization of Exu, Yps, and Orb. In conclusion, as a decapping factor, dDcp1 is required not only for the degradation of *osk* mRNA during embryogenesis but also for its cytoplasmic transportation during oogenesis.

Results

dDcp1 Is a Posterior Group Gene

The *b53* mutation was recovered from a screen for zygotic lethal mutations with specific maternal effects. A *P* transposase-insensitive $cFRT^{2L2R}$ second chromosome (see details in Experimental Procedures) was used as the direct target for the P{lArB} and P{PZ} mutators on the X chromosome. Four hundred fifty-six independent insertions on the $cFRT^{2L2R}$ chromosome were obtained from 768 P{lArB} and 232 P{PZ} transpositions. Among them, 113 homozygous lethal mutations were examined for their germline clone (GLC) phenotypes. The P{lArB}-induced *b53* mutation was isolated from the 46 lines with specific maternal effects.

Homozygous *b53* individuals show a pleiotropic lethal phase ranging from embryonic lethality to weakly surviving adults. Among embryos derived from females with *b53* germline clones, ~10% exhibit an abdominal deletions phenotype as well as deformed anterior structures when compared with wild-type (Oregon R) embryos (Figures 1A and 1B); the remaining 90% die before cuticle formation. The abdominal phenotype suggests that the *b53* mutation may affect a posterior group gene. Using inverse PCR and plasmid rescue, the position of the single $P\{lArB\}^{b53}$ insertion was determined (Figure 1J). After the *b53* chromosome was treated with transposase again, 52 viable wild-type revertants were recovered from 112 independent lines, thus confirming that the *b53* mutant phenotype is caused by the P element insertion.

The position of the P element insertion in the genomic sequence suggested that the *b53* mutant phenotypes may result from the disruption of *CG11183* and/or *CG5602*. Transgenic flies carrying different genomic fragments (T1–T5) were established (Figure 1J). Both the T1 and T2 fragments, which span the region containing *CG11183*, can fully rescue the *b53* mutant phenotypes (see Table S1 in the Supplemental Data available with this article online). This suggests that *CG11183*, but not *CG5602*, is most likely disrupted by the P insertion, as *CG5602* is not completely contained within the T2 fragment (Figure 1J). Unexpectedly, the *T3* transgene, which contains both the full-length *CG5602* and a truncation of *CG11183*, is able to rescue the lethality of the *b53* mutation. However, the rescued *b53/b53;T3/MKRS* flies show partial female sterility with a typical posterior group embryonic phenotype (Figure 1C and see below). From these results, we conclude that the posterior group embryonic phenotype of the *b53* mutation is caused by the P element-mediated disruption of the *CG11183* gene.

We further evaluated the origin of the lethality associated with *b53*. We reasoned that the rescue of the *b53* lethality by the *T3* transgene may be due to the 22 kDa N-terminal polypeptide of CG11183 contained within the transgene (Figures 1J and 1K and see below). To test this possibility, we constructed T4, which contains a BsiWI frameshift mutation that eliminates the 22 kDa polypeptide produced in T3 (Figure 1J). As expected, this transgene cannot rescue the *b53* lethality, although a few barely viable but sterile adult homozygous flies can survive (Table S1). We also constructed T5, which contains an NheI frameshift mutation that disrupts the CG5602 coding sequence in T3 (Figure 1J). T5 is expected to produce the 22 kDa polypeptide of CG11183 and a truncated form of the CG5602 protein. The *T5* transgene rescues the *b53* lethality, but the rescued females show a partial female sterility (Table S1). These data indicate that, although the 22 kDa N-terminal polypeptide of CG11183 can rescue both the lethality and the anterior phenotype, a possible effect of the *b53* mutation on *CG5602* cannot be ruled out. Based on these results, we confirm that the disruption of *CG11183*, but not *CG5602*, is responsible for the posterior group phenotype of the *b53* mutation.

A search of the databases revealed that the N-terminal 140 amino acids of CG11183 are highly conserved with the decapping domains of decapping proteins such as Dcp1p in *S. cerevisiae* and hDcp1a and hDcp1b in human (Figure 2A). However, their carboxy-terminal regions are less conserved (Figure 2B). These homologs all contain a putative EVH1/WH1 domain (Figure 2A) which is a protein-protein interaction module (Ball et al., 2002). Because CG11183 is the only Dcp1 homolog in the *Drosophila* genome, we refer to it as *Drosophila* decapping protein 1, or dDcp1.

The *b53/b53;T3/MKRS* individuals show a partial female sterile phenotype, with 60% of the embryos failing to hatch. Among the unhatched embryos, more than 90% show a typical posterior group phenotype (Figure 1C) and the remaining 10% have a minor posterior group phenotype. In addition to the abdominal phenotype, the pole cells are reduced in number (Figures 1F and 1G) or totally missing (Figures 1H and 1I) compared with wild-type (Figures 1D and 1E). This *b53/b53;T3/MKRS* phenotype can be defined as due to the effect of the P element insertion specifically on *CG11183*, after eliminating the possible effect on *CG5602* in the *b53* chromosome, because the whole transcription unit of *CG5602* is included in the T3 fragment (Figure 1J). In addition, the *T3* transgene in a wild-type background does not generate any mutant phenotypes, suggesting that the posterior group embryonic phenotype observed in *b53/b53;T3/MKRS* individuals is not caused by any dominant-negative effects of the N-terminal 22 kDa polypeptide of CG11183 (Figure 1K). This view is further strengthened by the absence of an embryonic phenotype when a 180 amino acid-containing N-terminal fragment of dDcp1 was expressed by *nanos-Gal4*-driven *UASp-N180* (Figure 1J). Hence, the *b53/b53;T3/MKRS* genotype provides a genetic background to specifically and easily analyze the posterior group phenotype of the *b53* mutation. To simplify our description, we define the

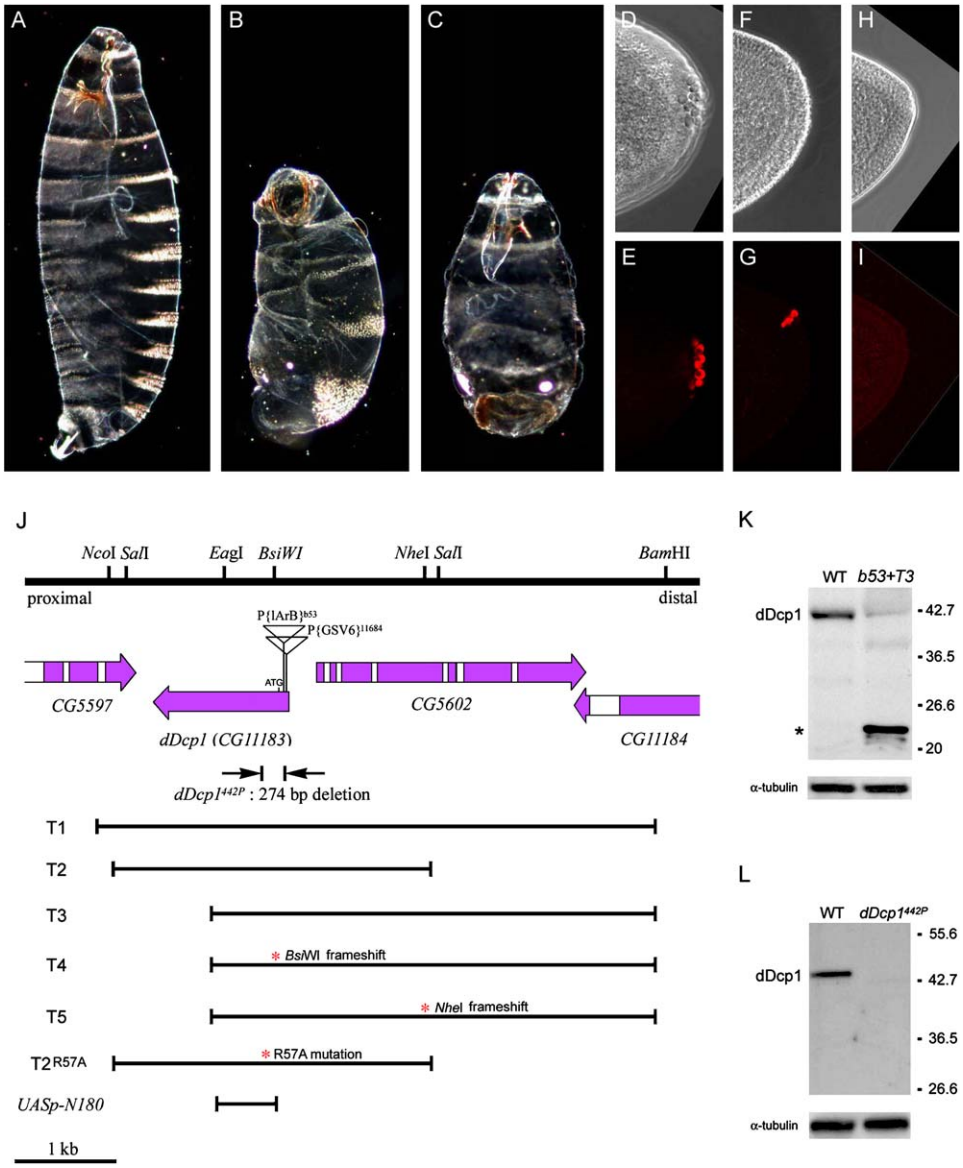

Figure 1. Mutant Phenotypes and Molecular Organization of the *dDcp1* Gene

(A–C) Embryonic cuticle preparations. (A) Wild-type embryo showing eight abdominal segments and an intact anterior region. (B) Both a deformed anterior region and abdominal deletions can be seen in a *b53* GLC embryo. (C) A typical abdominal deletion in a *b53+T3* embryo.

(D–I) The embryonic pole cells at cellular blastoderm stained with anti-Vasa antibody (red). Compared with wild-type (D and E), the pole cells are reduced in number or completely missing in *b53+T3* embryos (F–I). (D, F, and H) DIC images. (E, G, and I) Confocal images.

(J) Schematic representation of the *dDcp1* (*CG11183*) locus at polytene band 60A8, showing related genomic fragments and mutant alleles. The P{lArB}^{b53} insertion is 46 bp downstream of the transcription start site and 27 bp upstream of the translation start site of *CG11183*, and 318 bp upstream of the oppositely oriented *CG5602*. P{GSV6}^{11684} is located 35 bp upstream of the translation start site of *CG11183*. The deleted region in *dDcp1*^{442P} is shown. The T1–T5 and T2^{R57A} transgenic fragments for complementation tests and related experiments, as well as the UASp-N180 transgene, are shown.

(K and L) Western blot analyses. dDcp1 antibody specifically recognizes a 42 kDa band in wild-type extracts. (K) In a *b53+T3* ovarian extract, the 42 kDa band is barely visible and a 22 kDa band corresponding to the N-terminal dDcp1 polypeptide encompassed by the *T3* transgene is marked by an asterisk. (L) The 42 kDa band cannot be detected in a *dDcp1*^{442P} larval extract. α-tubulin was used as a loading control.

b53/b53;T3/MKRS genotype as "*b53* + *T3*" throughout this paper.

Because there is still a residual amount of full-length dDcp1 protein detectable in *b53+T3* (Figure 1K), a null allele is necessary for further analysis. From 450 imprecisely excised P{GSV6}^{11684} chromosomes, a dDcp1 protein null allele, *dDcp1*^{442P}, was recovered. *dDcp1*^{442P} has a 274 bp deletion, within which a fragment of 28 bases of unknown origin was inserted, extending from −27 to +247 bp with respect to the translation start site (Figures 1J and 1L). *dDcp1*^{442P} homozygous individuals die as early pupae, and this lethality can be rescued by the *T2* transgene. It is difficult to examine *osk* mRNA deposition in the *dDcp1*^{442P} background because *dDcp1*^{442P} GLC females produce egg chambers that arrest by stage 6 (data not shown). We therefore describe the

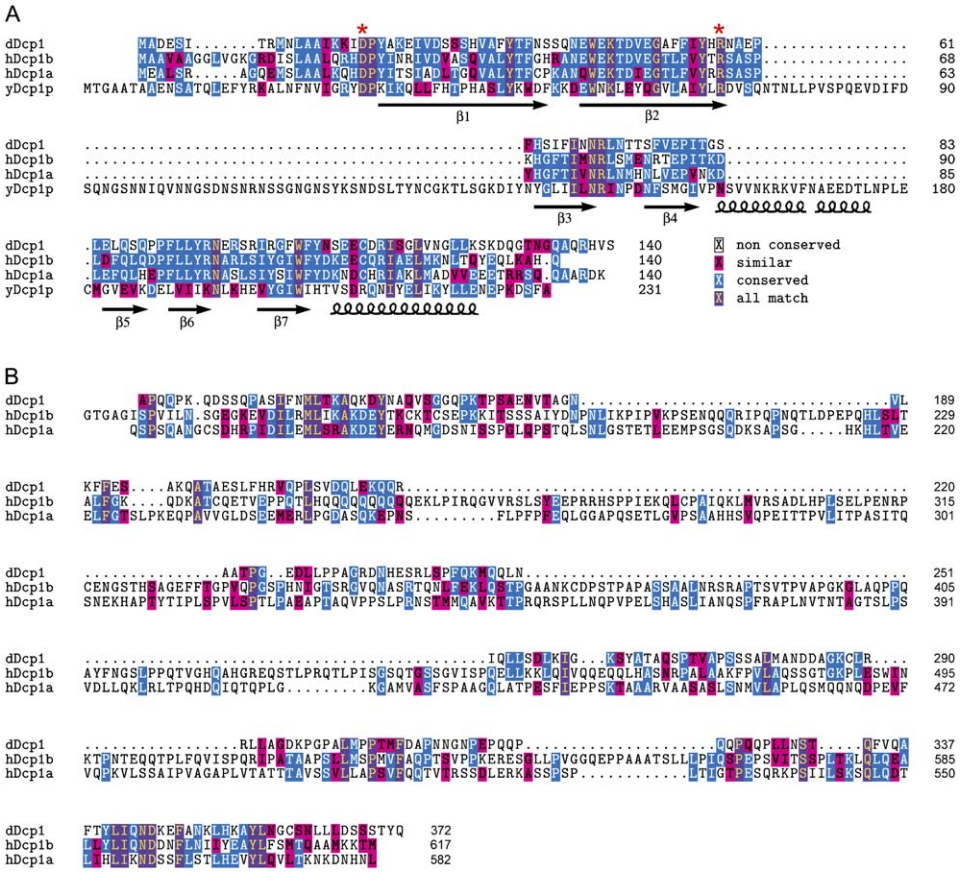

Figure 2. Sequence Alignment of dDcp1, hDcp1a, hDcp1b, and Dcp1p Decapping Proteins

(A) The N-terminal 140 amino acids of dDcp1, hDcp1a, and hDcp1b are conserved with full-length yeast Dcp1p. Conserved residues critical for decapping function (D18 and R57) in Dcp1 are marked with asterisks. Seven β sheets and an α helix that form the EVH1/WH1 domain in Dcp1p are indicated (She et al., 2004).

(B) The carboxy-terminal regions of dDcp1, hDcp1a, and hDcp1b are less well conserved.

dDcp1 mutant phenotypes based on the *b53* mutation and *b53+T3*.

dDcp1 Is Required for *osk* mRNA Degradation

The yeast Dcp1p decapping protein is an essential component of the 5′ to 3′ mRNA decay pathway. Loss of Dcp1p leads to a complete block of decapping in vivo (Beelman et al., 1996). The function of dDcp1 in mRNA decay is supported by the genetic requirement for *dDcp1* in the degradation of *osk* and other maternal mRNAs that were tested. In wild-type, the amount of *osk* mRNA is greatly reduced at 2–3 hr after egg laying (AEL) (Kim-Ha et al., 1991; Figure 3A1). In contrast, *osk* mRNA is more stable and can still be detected 4–5 hr AEL in *b53* GLC embryos (Figure 3A2). This mRNA degradation defect is most likely caused by the loss of dDcp1 because the lethality of the *b53* mutation can be rescued by the *dDcp1* wild-type transgene, *T2* (see above). Should CG5602 be responsible for the mRNA degradation defect, we would expect a complete rescue of this phenotype in *b53+T3*, which contains a wild-type *CG5602* transcript (Figure 1J). However, *osk* mRNA can still clearly be detected 3–4 hr AEL in *b53+T3* (Figure 3A3). But, the levels of mRNA detected are much less than those in *b53* GLC embryos. This partial rescue of the *osk* mRNA degradation defect suggests that disruption of *CG5602* is not the cause of the defect. In contrast, the *T2* transgene containing the full-length *CG11183* gene (Figure 1J) can completely rescue the delayed mRNA degradation phenotype in the *b53* mutation (Figure 3A4). We have therefore confirmed that the *dDcp1* mutation is responsible for the delayed *osk* mRNA degradation phenotype in *b53* GLC embryos.

The partially rescued degradation defect observed in *b53+T3* may be due to the presence of the 22 kDa N-terminal polypeptide of dDcp1 (Figure 1K), whose amino acid sequence is highly conserved with the decapping domains in the N-terminal regions of Dcp1 protein homologs (Figure 2A). To show that the putative decapping function of dDcp1 is required for the proper decay of *osk* mRNA, the R57 amino acid of dDcp1, which corresponds to a residue previously shown to be critical for Dcp1p and hDcp1a decapping activity (Tharun and Parker, 1999; Lykke-Andersen, 2002), was mutated to test its effect on *osk* mRNA degradation. We engineered an altered T2 fragment containing a dDcp1 coding sequence with an R57A substitution (Figure 1J). This $T2^{R57A}$ transgene does not show any mutant phenotype in a wild-type background, indicating that the R57A mutation does not cause any dominant-negative effects. In

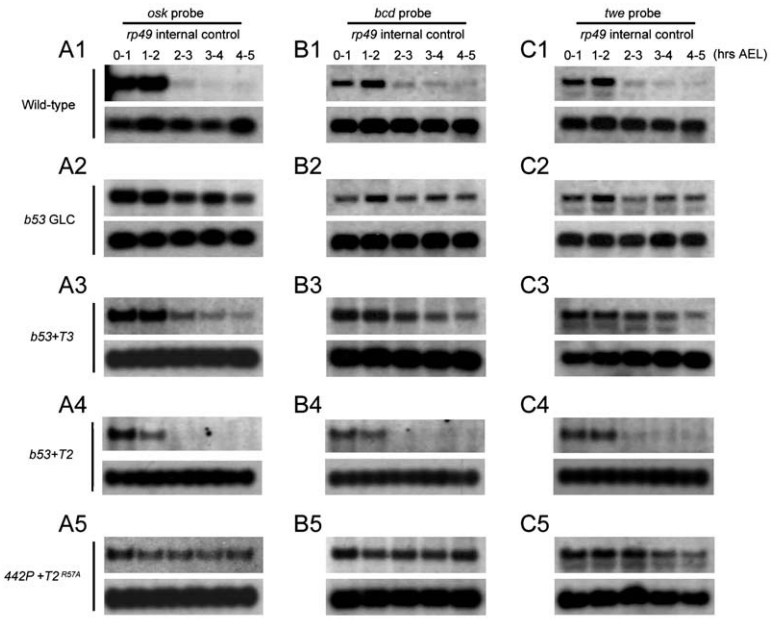

Figure 3. *dDcp1* Is Required for Maternal mRNA Degradation in Early Embryogenesis

Northern blot analyses using *osk* (A1–A5), *bcd* (B1–B5), and *twe* (C1–C5) probes.

(A1, B1, and C1) Normal maternal mRNA degradation in wild-type embryos. (A1) *osk*, (B1) *bcd*, and (C1) *twe* mRNAs are greatly reduced at 2–3 hr AEL.

(A2, B2, and C2) The degradation of maternal mRNAs is impaired in *b53* GLC embryos. (A2) *osk*, (B2) *bcd*, and (C2) *twe* mRNAs remain stable at 4–5 hr AEL.

(A3, B3, and C3) The degradation defects in *b53* GLC embryos are partially rescued by the *T3* transgene. (A3) *osk*, (B3) *bcd*, and (C3) *twe* mRNAs can be detected at 3–4 hr AEL in *b53+T3* embryos, at least.

(A4, B4, and C4) The degradation defects in *b53* GLC embryos are completely rescued by the *T2* transgene. (A4) *osk*, (B4) *bcd*, and (C4) *twe* mRNAs show extensive degradation at 2–3 hr AEL in *b53+T2* embryos.

(A5, B5, and C5) The degradation of maternal mRNAs is impaired in *442P+T2*^{R57A} embryos. (A5) *osk*, (B5) *bcd*, and (C5) *twe* mRNAs remain stable at 4–5 hr AEL. *rp49* mRNA is used as an internal loading control. One microgram of total embryonic RNA collected at 1 hr intervals was loaded in each lane. Genotype abbreviations: *b53+T3*: b53/b53;T3/MKRS, *b53+T2*: b53/b53; T2/MKRS, *442P+T2*^{R57A}: dDcp1^{442P}/dDcp1^{442P}; T2^{R57A}/MKRS.

addition, the levels of dDcp1^{R57A} protein produced in *dDcp1*^{442P}/*dDcp1*^{442P}; *T2*^{R57A}/*T2*^{R57A} ovaries are comparable to the wild-type dDcp1 protein levels (data not shown). This suggests that the dDcp1^{R57A} protein is stable when expressed. We therefore introduced the *T2*^{R57A} transgene into the *dDcp1*^{442P} null background to determine whether the R57A single amino acid substitution in dDcp1 is responsible for the *osk* mRNA degradation defect. Our results show that *osk* mRNA in *dDcp1*^{442P}/*dDcp1*^{442P}; *T2*^{R57A}/*MKRS* embryos can still be detected at 4–5 hr AEL (Figure 3A5), thus supporting the idea that the decapping function of dDcp1 is responsible for the regulation of *osk* mRNA degradation in embryogenesis. We conclude that *dDcp1* is a posterior group gene required for the proper degradation of *osk* mRNA.

We wanted to determine whether the degradation function of dDcp1 is specific to *osk*. To test this, we examined the degradation of both *bicoid* (*bcd*), the anterior determinant (Berleth et al., 1988), and *twine* (*twe*), the *cdc25* homolog uniformly distributed in the cytoplasm of the early embryo (Alphey et al., 1992). These two mRNAs are dramatically degraded at 2–3 hr AEL in wild-type embryos (Edgar and Datar, 1996; Surdej and Jacobs-Lorena, 1998; Figures 3B1 and 3C1). In *b53* GLC embryos, both *bcd* and *twe* mRNAs can still be detected 4–5 hr AEL (Figures 3B2 and 3C2). This degradation defect can be partially rescued in *b53* + *T3* embryos (Figures 3B3 and 3C3) but can be fully rescued in *b53+T2* embryos (Figures 3B4 and 3C4). mRNA degradation defects are also apparent in the *dDcp1*^{442P} null background containing the *T2*^{R57A} transgene, with both the *bcd* and *twe* mRNAs clearly detectable at 4–5 hr AEL (Figures 3B5 and 3C5). Thus, dDcp1 is required for the proper degradation of *bcd* and *twe* mRNAs and functions as a general degradation factor for maternal mRNAs.

dDcp1 Is Localized at the Posterior Pole of the Oocyte

A polyclonal dDcp1 peptide antibody was generated which recognizes an expected 42 kDa band in a Western blot of protein extracts from wild-type ovaries (Figure 1K). In the ovarian protein extracts of *b53+T3*, trace amounts of the 42 kDa band, as well as an extra 22 kDa band, were detected (Figure 1K). The 22 kDa band represents the N-terminal 185 amino acids of dDcp1 produced by the *T3* transgene (Figure 1J). In *dDcp1*^{442P}, the 42 kDa band is undetectable in a larval extract (Figure 1L). After stage 2 of oogenesis, dDcp1 protein is localized at the posterior pole of the oocyte until stage 7 (Figures 4A–4C). At stage 8, dDcp1 transiently accumulates at the anterior pole of the oocyte and forms a ring structure (Figure 4D). This transient anterior accumulation pattern is similar to that of *osk* mRNA (Ephrussi et al., 1991; Kim-Ha et al., 1991) and other posteriorly localized components, such as Yps (Wilhelm et al., 2000) and Btz (van Eeden et al., 2001). After stage 9, dDcp1 is relocalized at the posterior crescent and is maintained there until at least stage 10B (Figures 4E and 4F). This dDcp1 staining pattern was reconfirmed using an HA-tagged dDcp1 fusion protein (Figures 4G–4I).

dDcp1 Colocalizes with dDcp2 and Me31B in the Nurse Cell Cytoplasm

The punctate staining of dDcp1 in the nurse cell cytoplasm is particularly obvious, especially at early stages (Figures 4A–4C). These discrete cytoplasmic foci are

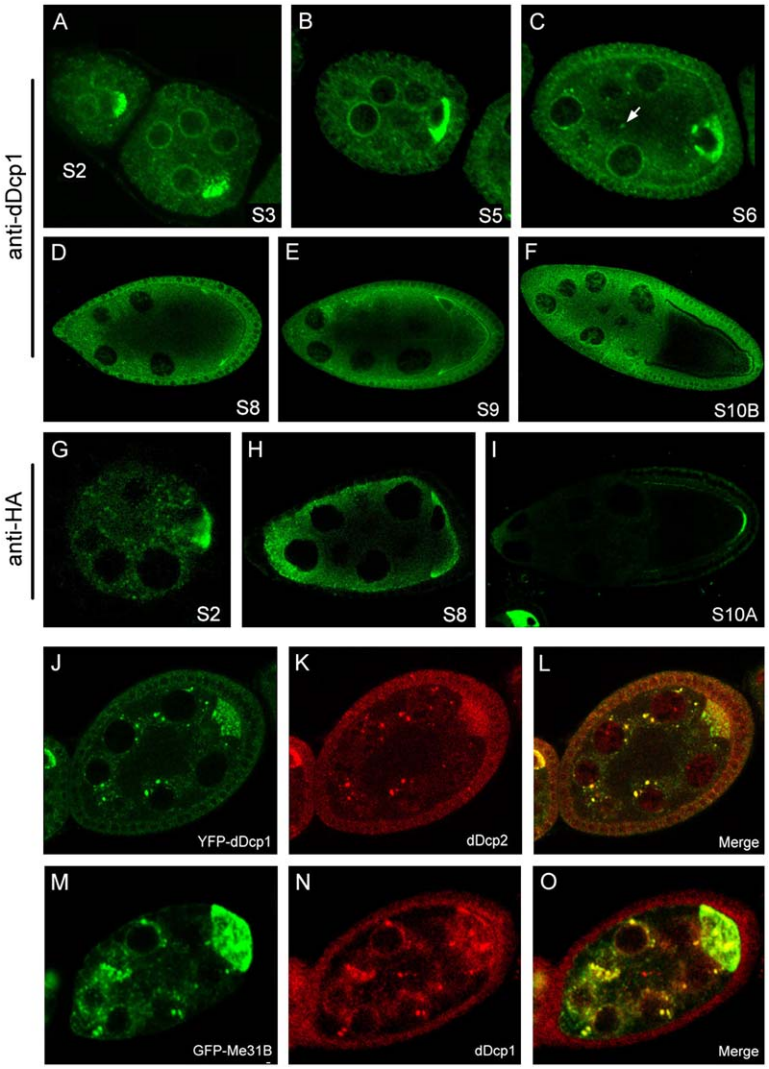

Figure 4. Distribution of dDcp1 during Oogenesis

(A–F) Distribution pattern of dDcp1 in wild-type egg chambers. In the oocyte, dDcp1 accumulates at the posterior end at (A) stages 2 and 3, (B) stage 5, and (C) stage 6. At (D) stage 8, dDcp1 is transiently localized at the anterior end of the oocyte. At (E) stage 9 and (F) stage 10, dDcp1 is localized to the posterior pole of the oocyte. In nurse cells, dDcp1 can also be detected in discrete cytoplasmic foci (arrow) at early stages (A–C).

(G–I) HA antibody staining in (G) stage 2, (H) stage 8, and (I) stage 10A *nanos-Gal4VP16*; *UASp-HA-dDcp1* egg chambers.

(J–L) A stage 7 egg chamber expressing YFP-dDcp1 was double stained for YFP (green) and dDcp2 (red).

(M–O) A stage 7 egg chamber expressing GFP-Me31B was double stained for GFP (green) and dDcp1 (red).

more visible in HA-dDcp1 (Figure 4G) and YFP-dDcp1 (Figure 4J) egg chambers and conspicuously resemble the descriptions of P bodies (Sheth and Parker, 2003; Cougot et al., 2004). We first examined whether dDcp1 can colocalize with *Drosophila* Dcp2 (dDcp2), encoded by CG6169, using a dDcp2 antibody (see Experimental Procedures). From early stages up to stages 8–9, the dDcp2 antibody is able to recognize discrete sites in both the cytoplasm and nuclei of nurse cells (Figures S1A–S1C). At stage 10, dDcp2 cytoplasmic foci in the nurse cells are greatly reduced, and staining is concentrated mainly in the nucleus. However, there is no enrichment of dDcp2 at the posterior pole of the oocyte (Figure S1D). These punctate foci of dDcp2 staining in the nurse cell cytoplasm are greatly reduced in dDcp2 RNAi egg chambers, indicating that this antibody specifically recognizes dDcp2 in nurse cells (Figures S1E and S1F). As expected, YFP-dDcp1 colocalizes with the discrete dDcp2 particles in the nurse cell cytoplasm (Figures 4J–4L). Furthermore, we also found that dDcp1 can colocalize with GFP-Me31B in the nurse cell cytoplasm (Figures 4M–4O). From these results, we propose that these dDcp1/dDcp2/Me31B particles are the putative P bodies in the nurse cell cytoplasm.

dDcp1 Specifically Affects the Posterior Deposition of *osk* mRNA

In wild-type oocytes, *osk* mRNA is localized at the posterior crescent (Figure 5A) and *bcd* mRNA forms an anterior ring structure (Figure 5C) at stage 10. In about 40% of *b53* GLC egg chambers, *osk* mRNA fails to localize properly at the posterior pole, and in some cases *osk* accumulates in nurse cells and at the anterior pole of the oocyte (Figure 5B). However, localization of *bcd* mRNA is not affected (Figure 5D). Gurken (Grk), the determinant of dorsal follicle cell fate (Nilson and Schupbach, 1999), is localized to the anteriodorsal corner in wild-type oocytes (Figure 1E). Its distribution pattern is not affected in *b53* + *T3* egg chambers (Figure 5F). Because both abdomen and pole cell formation are affected in *dDcp1* mutant embryos, *dDcp1* would be predicted to be a posterior group gene (reviewed in van Eeden and St Johnston, 1999). We thus further examined the expression patterns of Stau, Osk, and Vasa in the *b53* + *T3* background. In wild-type oocytes, Stau, Osk, and Vasa all accumulate in a crescent that is tightly localized to the posterior pole of the oocyte after stage 9 (Figures 5G, 5I, and 5K). By contrast, in ~60% of stage 9-10 mutant egg chambers, the posterior localization of Stau is reduced

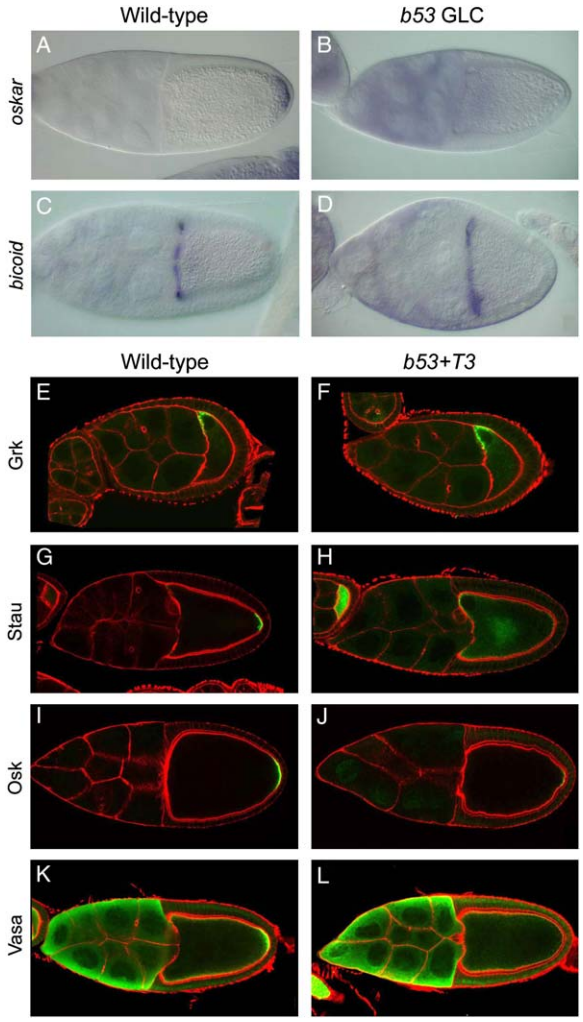

Figure 5. Mutations in *dDcp1* Specifically Affect the Posterior Deposition of Maternal Determinants

(A–D) In situ hybridization of (A and B) *osk* and (C and D) *bcd* mRNA in stage 10 egg chambers. The posterior localization of *osk* mRNA is disrupted in a *b53* GLC oocyte (B). The anterior localization of *bcd* mRNA is unaffected in a *b53* GLC oocyte (D).

(E–L) Immunostaining in stage 9-10 egg chambers. Compared with the wild-type control (E), the anterior-dorsal Grk distribution is unaffected in a *b53+T3* oocyte (F). Compared with wild-type controls (G, I, and K), the posterior localization of (H) Stau, (J) Osk, and (L) Vasa is reduced or lost in b53+T3 oocytes. Note that in some cases, a faint and diffuse Stau staining (H) can be detected in the *b53+T3* oocyte. The cell boundary was marked by Texas red phalloidin (red).

or totally diminished. In some cases, Stau can be detected faintly and diffusely in the middle ooplasm and accumulates at the anterior cortex (Figure 5H). Osk and Vasa staining is also dramatically reduced at the posterior (Figures 5J and 5L). Moreover, dDcp1 does not cause the precocious translation of *osk* mRNA (data not shown). Collectively, these results indicate that *dDcp1* is a posterior group gene specifically required for the posterior deposition of *osk* mRNA.

The Localization of dDcp1 Is Dependent on *osk* mRNA as Well as on Microtubule Organization

Because dDcp1 is required for the proper degradation of several maternal mRNAs during embryogenesis (Figure 3), it is possible that dDcp1 affects the posterior localization of *osk* indirectly via its decapping function. However, the R57A single amino acid substitution in the decapping domain of dDcp1 does not disrupt the posterior localization of *osk* mRNA in any egg chambers examined (Figures S2A and S2B). Compared with wild-type, the partially sterile $dDcp1^{442P}/dDcp1^{442P}$; $T2^{R57A}$/*MKRS* females (Table S1) do not show defects in pole cell formation (Figures S2C–S2F) and do not have a grandchildless phenotype. These observations clearly rule out the above-mentioned possibility. Furthermore, in *dDcp1* mutations, the mislocalization of *osk* mRNA could be an indirect consequence of the disorganization of the microtubule network or reflect a direct requirement for dDcp1 for the proper formation of the *osk* mRNP transportation complex. To investigate whether microtubule cytoskeletal orientation is affected by dDcp1, we examined the microtubule plus end using Kinesin-lacZ (Clark et al., 1994) and the minus end using Centrosomin (Li and Kaufman, 1996). Overall microtubule organization and integrity were studied by examining the distribution of the microtubule binding protein Tau-GFP (Micklem et al., 1997). In the *b53+T3* oocyte, posterior localization of Kinesin-lacZ (Figure S3B) and localization of Centrosomin at the anterior cortex (Figure S3D), as well as the distribution pattern of Tau-GFP (Figure S3F), are indistinguishable from wild-type (Figures S3A, S3C, and S3E). Obviously, the requirement of dDcp1 for *osk* mRNA posterior localization is not due to an indirect effect on microtubule organization. Taking all of these data together, it is more likely that dDcp1 is directly involved in formation of the *osk* mRNP complex.

Stau, a dsRNA binding protein, interacts with *osk* mRNA and directs its posterior deposition (Ramos et al., 2000). It functions as an adaptor to transport *osk* in a Khc-dependent manner (Brendza et al., 2000). As suspected, HA-dDcp1 is colocalized with Stau at the posterior end of the oocyte, and this colocalization is maintained until at least stage 10 (Figures 6A–6C). In both khc^{27} GLC and $stau^{D3}$ mutant egg chambers, dDcp1 is no longer localized to the posterior end and instead accumulates at the anterior pole and the lateral cortex of the oocyte (Figures 6D and 6E). This altered spatial accumulation of dDcp1 in a *khc* mutant background is quite similar to that of *osk* mRNA (Brendza et al., 2000). Should dDcp1 indeed be a component of the *osk* mRNP complex, its level at the posterior pole should be dependent on the dosage of *osk*. This was confirmed by the excessive posterior localization of dDcp1 in a genetic background containing two extra copies of *osk* genomic sequences (Figure 6F). These data further support the hypothesis that dDcp1 is a component of the *osk* mRNP complex. As a component of this complex, the localization of dDcp1 should be *osk* mRNA dependent. This was shown by the anterior accumulation of dDcp1 when *osk* mRNA was ectopically localized to the anterior pole using an *osk-bcd*-3′UTR hybrid mRNA (Figure 6G; Ephrussi and Lehmann, 1992). In both grk^{2B6}/grk^{HF48} and $par\text{-}1^{6821}/par\text{-}1^{6323}$ mutant combinations, *osk* mRNA is mislocalized to the center of the oocyte due to misorientation of the microtubule network (Gonzalez-Reyes et al., 1995; Shulman et al., 2000). In a grk^{2B6}/grk^{HF48} mutant background, dDcp1 can be deposited in the middle of the oocyte in

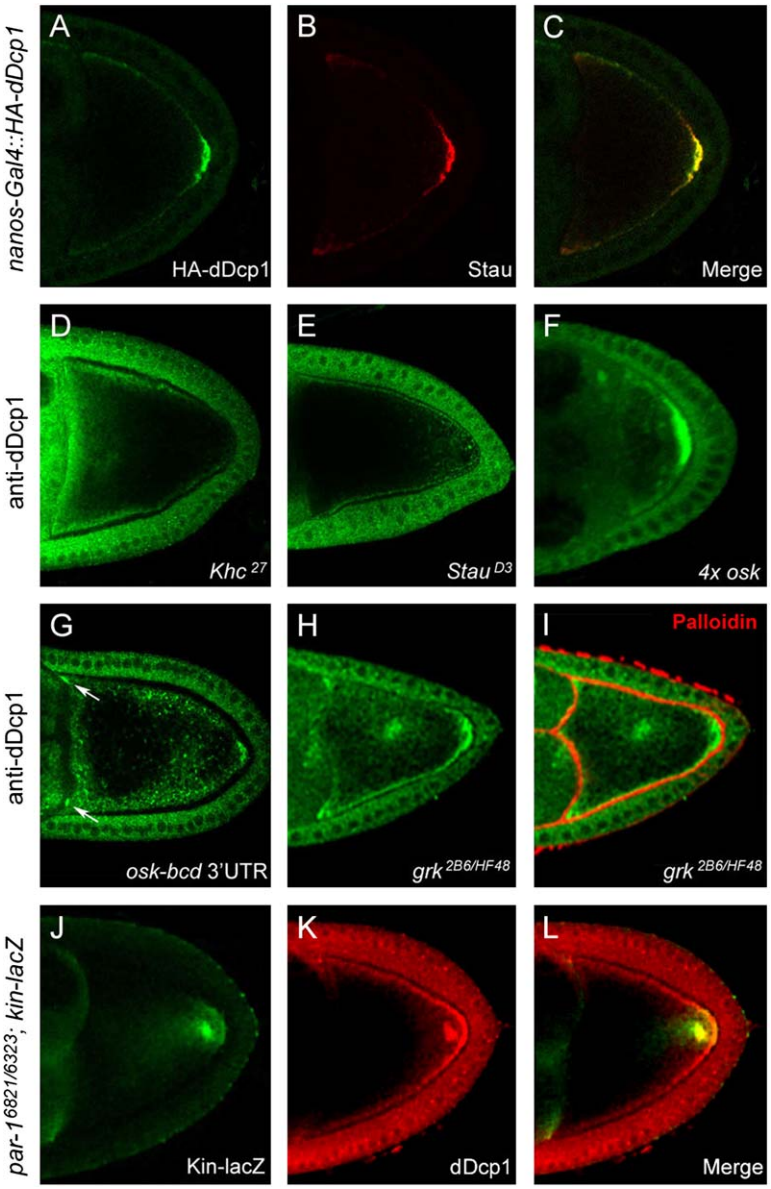

Figure 6. The Posterior Localization of dDcp1 Is *osk* mRNA Dosage and Position Dependent, and Microtubule Organization Dependent

(A–C) HA-dDcp1 (green) (A) is colocalized with Stau (red) (B) in the posterior crescent of the *nanos-Gal4VP16*; *UAS-HA-dDcp1* oocyte.

(D and E) dDcp1 (green) accumulates in the anterior and lateral cortex in (D) khc^{27} GLC and (E) $stau^{D3}$ oocytes.

(F) The posterior localization of dDcp1 (green) is increased in an oocyte carrying four copies of the *osk* gene.

(G) dDcp1 (green) is ectopically localized to the anterior (arrows) of an *osk-bcd 3′UTR* oocyte.

(H and I) dDcp1 (green) is mislocalized in grk^{2B6}/grk^{HF48} oocytes. The cell boundary is marked by Texas red phalloidin (red) (I).

(J–L) dDcp1 (red) is mislocalized in $par\text{-}1^{6821}/par\text{-}1^{6323}$; *kin-lacZ*/+ oocytes. The microtubule plus end is labeled by Kinesin-lacZ (green, anti-lacZ) (J and L).

HA-dDcp1 was detected by rat anti-HA antibody (A and C). dDcp1 was detected by rabbit anti-dDcp1 antibody (D–I, K, and L). Stage 9-10 egg chambers are shown in all panels.

the same way as *osk* mRNA (Figures 6H and 6I). Similarly, in $par\text{-}1^{6821}/par\text{-}1^{6323}$ mutant oocytes, dDcp1 is mislocalized and colocalizes with a Kinesin-lacZ fusion protein marking the plus end of microtubules (Figures 6J–6L). Altogether, these data clearly indicate that the localization of dDcp1 is dependent on the organization of microtubules and is determined by the position of *osk* mRNA, which is similar to the behavior of other *osk* mRNP complex components.

dDcp1 Is Required for the Posterior Localization of Exu, Yps, and Orb

Among those proteins involved in *osk* mRNA localization, Exu and dDcp1 have a similar spatial and temporal distribution pattern in both nurse cells and the oocyte. In the oocyte, each accumulates transiently at the anterior pole and subsequently becomes localized to the posterior pole (Mansfield et al., 2002; Figures 4D–4F). We therefore suspected that dDcp1 can interact with Exu and thus would be a new component of the large Exu-Yps mRNP complex. As expected, dDcp1 colocalizes with GFP-Exu in the posterior pole of the stage 10 oocyte (Figures 7A–7C). In addition, the punctate pattern of dDcp1 clearly matches that of GFP-Exu in the nurse cell cytoplasm of stage 9 egg chambers (Figures 7D–7F). Exu is known to be a component of sponge bodies, which are subcellular structures consisting of RNA and ER-like cisternae embedded in an amorphous electron-dense mass (Wilsch-Brauninger et al., 1997). Taken together with the facts that Exu colocalizes with dDcp1 (Figures 7D–7F) and dDcp1 colocalizes with both dDcp2 and Me31B (Figures 4J–4O), it will be interesting to clarify whether the previously identified sponge bodies are the putative P bodies in the nurse cell cytoplasm.

Genetically, dDcp1 is required for the posterior localization of Exu and Yps. In a *b53+T3* background, the posterior localization of GFP-Exu after stage 9 is impaired (Figure 7M). Instead of its normal posterior localization, Yps accumulates excessively at the anterior pole in stage 10 *b53+T3* oocytes (Figures 7K and 7N).

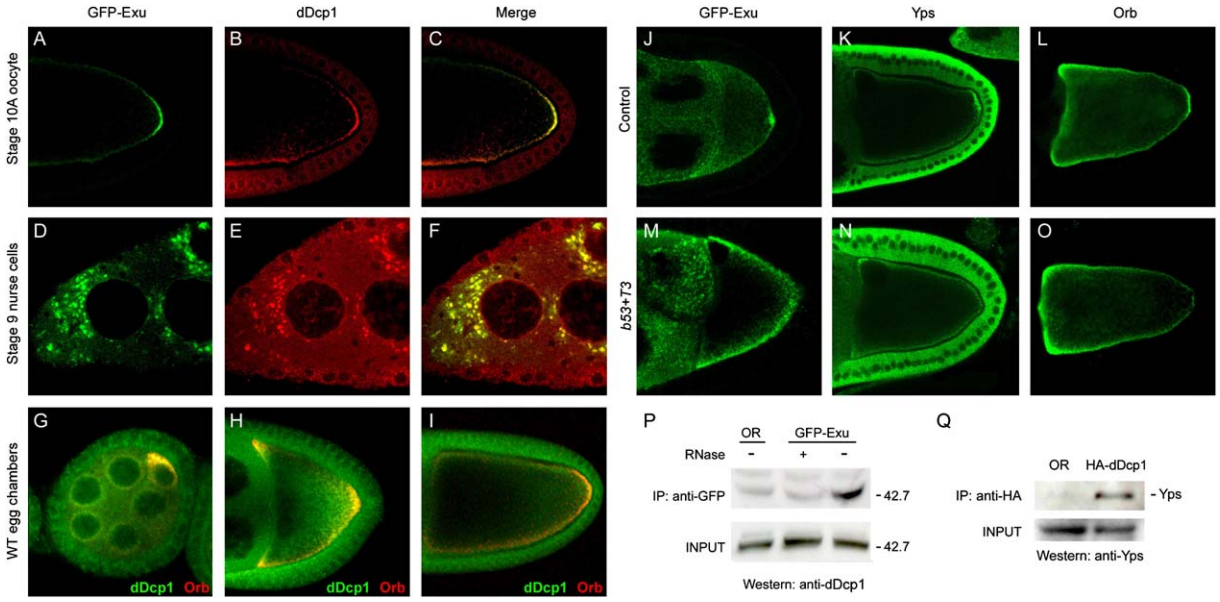

Figure 7. dDcp1 Interacts with Exu and Yps and Is Required for the Posterior Localization of Exu, Yps, and Orb

(A–F) dDcp1 (red) is colocalized with GFP-Exu (green) in (A–C) the posterior end of the oocyte and (D–F) the cytoplasm of nurse cells.

(G–I) dDcp1 (green) is colocalized with Orb (red) at the posterior end of the oocyte in (G) stage 5, (H) stage 9, and (I) stage 10 egg chambers. In addition, in early stage 9 egg chambers (H), dDcp1 is also colocalized with Orb at the anterior end of the oocyte.

(J–O) Compared with wild-type controls (J–L), the posterior localization of GFP-Exu (stage 9), Yps (stage 10), and Orb (stage 10) is disrupted in *b53+T3* mutant oocytes (M–O). Genotype used in (M): *b53/b53*; *T3/GFP-Exu*.

(P) GFP-Exu coimmunoprecipitates with dDcp1 in an RNase-sensitive manner. A GFP-Exu ovarian extract was immunoprecipitated using an anti-GFP antibody. Western blotting was performed using an anti-dDcp1 antibody.

(Q) HA-dDcp1 coimmunoprecipitates with Yps. Ovarian extract from *α4-tubulinGal4VP16*; *HA-dDcp1* females was immunoprecipitated using an anti-HA antibody. Western blotting was performed using an anti-Yps antibody. In (P) and (Q), a wild-type (OR) ovarian extract was used as the control. The input was 1/100 the volume of the ovarian extract used in the coimmunoprecipitation reaction.

By contrast, the distribution patterns of Exu and Yps at earlier stages are not affected (data not shown). By coimmunoprecipitation, dDcp1 was found to interact with GFP-Exu (Figure 7P) in an RNase-sensitive manner. This RNase-sensitive interaction between dDcp1 and Exu indicates a complex nucleated on the RNA. Similarly, Yps can be coimmunoprecipitated with HA-dDcp1 (Figure 7Q). Combining the coimmunoprecipitation and genetic data (Figures 6 and 7), we propose that dDcp1 and Exu are in the same *osk* mRNP complex, given that the interaction between Exu and *osk* has been reported (Wilhelm et al., 2000). Together with the observation that dDcp1 is colocalized with Exu in both nurse cells and the oocyte during oogenesis (Figures 7A–7F), and the requirement of dDcp1 for proper Exu and Yps posterior localization (Figures 7M–7O), we conclude that dDcp1 is a component of the *osk*-Exu-Yps mRNP complex.

Orb interacts with Exu in an RNA-dependent manner and functionally antagonizes Yps (Mansfield et al., 2002). By coimmunostaining, dDcp1 was found to colocalize with Orb in the oocyte from early stages to stage 9 (Figures 7G and 7H). The posteriorly localized dDcp1 continues to colocalize with Orb after stage 9 (Figure 7I), although the anterior accumulation of dDcp1 is reduced. We further examined whether the posterior localization of Orb is also *dDcp1* dependent. At stage 9, dDcp1 and Orb remain colocalized in *b53+T3* mutant egg chambers (data not shown). In the stage 10 mutant oocyte, Orb has less posterior staining and accumulates mostly at the anterior cortex (Figure 7O) compared with wild-type (Figure 7L). This implies that after stage 9, dDcp1 is required to recruit Orb into the posterior *osk* mRNP complex so that Orb can activate translation. Nevertheless, we cannot rule out the possibility that the recruitment of Orb is *osk* mRNP complex dependent. Altogether, these results provide evidence that dDcp1 in the *osk*-Exu-Yps mRNP complex contributes to the posterior localization of *osk* mRNA and is genetically required for the proper localization of Exu, Yps, and Orb.

Discussion

Our data reveal that the decapping factor dDcp1 is a component of the *osk* mRNP complex. As such, the presence of dDcp1 is expected to cause the degradation of *osk* mRNA. However, *osk* mRNA degradation seems to be repressed until embryogenesis. How can dDcp1 remain stably associated with its substrate without initiating mRNA decay? First, the presence of dDcp1 in the *osk* mRNA complex may be independent of the presence of dDcp2. Because it has been suggested that Dcp1 and Dcp2 function together in vivo in a decapping holoenzyme with Dcp2 as the catalytic subunit, Dcp1 alone should not constitute the active decapping machinery (Beelman et al., 1996; Van Dijk et al., 2002; Lykke-Andersen, 2002; Wang et al., 2002; Steiger et al., 2003). Our observation of the lack of dDcp2 posterior crescent staining in the oocyte after stage 9 supports this possibility (Figures S1C and S1D). Second,

the poly(A) tail and poly(A) binding proteins can be repressors of mRNA decay (Coller et al., 1998; Wilusz et al., 2001; Khanna and Kiledjian, 2004). This is supported by the observation that the length of the *osk* poly(A) tail ranges from 100 to 230(A) during its transportation (Chang et al., 1999; Castagnetti and Ephrussi, 2003). Third, eIF4E and the association of ribosomes on mRNA can inhibit decapping activity (Schwartz and Parker, 2000; Ramirez et al., 2002). During oogenesis, *osk* mRNA is associated with polysomes even if it is not yet posteriorly localized (Braat et al., 2004). This suggests that a stable translational initiation complex is preassembled with *osk* mRNA during its transportation and consequently may be able to repress the decapping function of dDcp1. These mechanisms may provide a plausible explanation of an inhibitory system acting during transportation and a degradation system that can be activated or derepressed only after *osk* mRNA is set for degradation at early embryogenesis.

Me31B, the *Drosophila* homolog of decapping activator Dhh1p in yeast, is involved in the translational repression of *osk* mRNA and interacts with Exu in an RNase-dependent manner (Nakamura et al., 2001). Dhh1p physically interacts with Dcp1p and stimulates mRNA decapping (Coller et al., 2001). Likewise, dDcp1 may interact with Me31B and repress the translation of *osk* mRNA. However, in the *b53* GLC and *b53* + *T3* egg chambers examined, we could not observe any premature translation of *osk* mRNA (data not shown). Although it is still not clear whether Me31B is also an activator for decapping, Me31B can colocalize with dDcp1 in discrete cytoplasmic foci in nurse cells (Figures 4M–4O). Moreover, Me31B has been found to colocalize with eIF4E and Cup (Wilhelm et al., 2003; Nakamura et al., 2004), whereas mammalian eIF4E and the mammalian homolog of Cup are located in P bodies (Ferraiuolo et al., 2005; Andrei et al., 2005). Because dDcp1 is required for the degradation of several maternal mRNAs (Figure 3) and is colocalized with dDcp2 (Figures 4J–4L), we suggest that these discrete cytoplasmic foci in nurse cells are the putative *Drosophila* P bodies. In addition to dDcp1, both Me31B and the polysomal apparatus are also components of the *osk* mRNP complex in the oocyte (Nakamura et al., 2001; Braat et al., 2004) and are components of the polar granules. Interestingly, their counterparts, Dcp1p/hDcp1a, Dhh1p/Rck, and eIF4E also reside in yeast and human P bodies (Sheth and Parker, 2003; Cougot et al., 2004). The presence of shared components suggests that polar granules and P bodies are closely related structures. This raises the possibility that a conversion between these two particles may exist during development.

Prior to localization, the translation of *osk* mRNA is repressed. After stage 9, its translation is derepressed at the posterior end of the oocyte. Considering the coexistence of the translational repressors and activators of *osk* mRNA at the posterior end of the oocyte at stage 10, it is possible that *osk* mRNA exists in a balance between translational repression and activation. Recently, activators of mRNA decapping such as yeast Dhh1p and mammalian RCK/p54 have been found to be translational repressors (Coller and Parker, 2005). These findings led to a model in which the translational status of a cytoplasmic mRNA is the consequence of competition between the translational apparatus and the repression apparatus (Coller and Parker, 2005). Furthermore, there is also a reciprocal movement of mRNAs between polysomes and P bodies (Brengues et al., 2005). A dynamic switch of mRNAs among translational activation, translational repression, and degradation is conceivable. Considering that both dDcp1 and Me31B are evolutionarily conserved decapping factors in P bodies and are present in *osk* mRNP at stage 10, we would expect that the status of *osk* mRNA can potentially shift from translation repression to degradation. Nevertheless, the majority of *osk* mRNA degradation occurs during early embryogenesis instead of during oogenesis (Ephrussi et al., 1991; Kim-Ha et al., 1991). Under these circumstances, the preassociation of the dDcp1/Me31B decapping factors on the *osk* mRNP complex is presumably not able to act as an active degradation machinery. Together with the fact that dDcp1 does not have a translational repression function during oogenesis, we propose that the existence of dDcp1/Me31B on the *osk* mRNP complex may contribute to the embryonic degradation of *osk* mRNA. One possibility is that an unknown factor can trigger the rapid degradation of *osk* mRNA at the maternal-zygotic transition in early embryogenesis, which is supported by the finding that Smaug is a trigger of maternal *hs83* mRNA degradation in embryos (Semotok et al., 2005). Instead of assembling a degradation complex de novo, the preincorporation of dDcp1/Me31B may facilitate the degradation of *osk* mRNA during the maternal-zygotic transition.

Experimental Procedures

Drosophila Stocks

The wild-type strain used is Oregon R (OR). Fly stocks were raised at 25°C on standard cornmeal and agar medium. The following transgenic stocks were used in this study: P{w+; *kinesin-LacZ* }^{KZ503} (Clark et al., 1994); P{w+; *Tau-GFP*} (Micklem et al., 1997); P{w+; *GFP-Exu*}^{NGE3} (Theurkauf and Hazelrigg, 1998); P{w+; *GFP-Me31B*} (Nakamura et al., 2001); *nanos-Gal4VP16* (Van Doren et al., 1998); *α4-tubulin-Gal4VP16* (a gift from N. Perrimon); P{*osk*$^{+}$6.45} (Ephrussi et al., 1991); P{*osk-bcd* 3′UTR} (Ephrussi and Lehmann, 1992); and *P{GSV6}*^{11684} (*Drosophila* Gene Search Project, Tokyo Metropolitan University). We also used the following mutant alleles: *stau*^{D3}, *par-1*^{6821}, and *par-1*^{6323} (Shulman et al., 2000); *khc*^{27} (Brendza et al., 2000); *grk*^{2B6} and *grk*^{HF48} (Neuman-Silberberg and Schupbach, 1993). All other stocks used were provided by the Bloomington Stock Center.

The *P* Transposase-Insensitive *cFRT*^{2L2R} Chromosome

The *FRT*^{2L2R} chromosome, containing P{hs-neo>>, ry^{+}, FRT}^{40A} on 2L and P{>w^{hs}>, FRT}^{42B} on 2R (Chou and Perrimon, 1996), was modified to become insensitive to *P* transposase after three consecutive transposase treatments. Four hundred twenty-seven independent *FRT*^{2L2R} chromosomes that showed no somatic transposition based on lack of mosaicism in the eye were selected after two challenges with *P* transposase. Among these, 107 homozygous viable lines with *rosy* eyes were recovered. These lines were then examined for their efficiency of germline clone (GLC) production. The number of ovaries with developed vitellogenic egg chambers versus the total number of ovaries was determined using the autosomal FLP-DFS technique (Chou and Perrimon, 1996). Based on this analysis, the two most efficient chromosomes, with a 55%–85% GLC efficiency for both the 2L and 2R arms, were selected for further treatment. One chromosome remained insensitive after further *P* transposase treatment, as its GLC efficiency ranged consistently from around 55% to 85% for both arms in ten independent homozygous viable progeny examined. The isogenized chromosome produced GLC-derived embryos that have a greater than 95% hatching

rate for both arms. Apparently, the repeated transposase challenge did not create detectable lesions in this particular chromosome.

Originally, P{hs-neo>>, ry^{+}, FRT}^{40A} was inserted 3′ to the T at position 240696 of the AE003781 clone, with the 3′ end of the P element closer to the centromere. In *clipped* P{hs-neo>>, ry^{+}, FRT}^{40A}, imprecise excision removes the 5′ end of the P element and most of the *rosy* coding sequences, that is, from base 26 to approximately base 2070 of P{neo FRT} (the FBtp0000348 locus according to FlyBase). P{>w^{hs}>, FRT}^{42B} was originally inserted 3′ to the T at position 11497 of the AE003789 clone, with the 5′ end of the P element closer to the telomere. In *clipped* P{>w^{hs}>, FRT}^{42B}, the 5′ end of the P element and one of the FRT repeats (bases 10–2821 of P{FRT(w^{hs})}, the FBtp0000268 locus according to FlyBase) were deleted. Because the 5′ region of the P element is necessary for transposition, neither *clipped* P{hs-neo>>, ry^{+}, FRT}^{40A} nor *clipped* P{>w^{hs}>, FRT}^{42B} can be mobilized using *P* transposase. Nevertheless, the FRT sequences are fully functional for FLP-driven site-specific recombination. Due to the clipping off of the respective 5′ regions of the P elements in the original chromosome, this new chromosome is termed *clipped FRT^{2L2R}*, or *cFRT^{2L2R}*. After P element mutagenesis of this chromosome, it is possible to generate local imprecise excision events to create new alleles of the P element-induced mutation of interest. Any such mutation induced on this chromosome can then be examined for its behavior in homozygous recombinant clones by the FLP-FRT site-specific recombination system. The *cFRT^{2L2}* chromosome is thus a useful tool for the systematic disruption and subsequent analysis of more than 35% of the fly genome.

Transgenes

The 5.4 kb NcoI-BamHI T1 genomic fragment, the 3 kb SalI-SalI T2 genomic fragment, and the 4.3 kb EagI-BamHI T3 genomic fragment from P1 clone DS06090 (obtained from the Berkeley *Drosophila* Genome Project) were each subcloned into pCaSpeR4 for complementation analysis (Figure 1J). The T4 genomic fragment was constructed by digestion of the T3 fragment with BsiWI followed by Klenow treatment and self-ligation. This generates a frameshift after the 11th amino acid in the N-terminal region of CG11183 in T4. The T5 genomic fragment was constructed by digestion of the T3 fragment with NheI followed by Klenow treatment and self-ligation. This generates a frameshift after the NheI site which disrupts the coding sequence of CG5602. The T2^{R57A} fragment, which contains an R to A substitution at amino acid 57 in dDcp (Figure 1J), was generated using a QuikChange site-directed mutagenesis kit (Stratagene). P{UASp-HA-dDcp1} and P{UASp-HA-N180-dDcp1} were generated by introducing the N-terminal HA-tagged full-length dDcp1 and an HA fusion of the N-terminal 180 amino acids of dDcp1, respectively, into pUASp. The dDcp1 full-length coding sequence was obtained from EST clone GH04763. To generate a YFP-dDcp1 fusion protein, the EYFP coding sequence (Clontech) was inserted directly in front of the translational start site of *dDcp1* in the 2.8 kb SalI-XbaI genomic fragment subcloned from T2.

Northern Blot Analysis

Total RNAs were extracted from staged embryo collections at 1 hr intervals from different *dDcp1* genotypes using the Purescript RNA Isolation kit (Gentra). DIG-labeled (Roche) *osk*, *bcd*, *twe*, and *rp49* RNA probes were made by in vitro transcription using the DIG Northern Starter kit (Roche). Please see Supplemental Data for cloning details of plasmids used for probe generation. Northern blot procedures were carried out using the Dig application manual for filter hybridization (Roche).

Antibody Generation and Immunochemistry

For dDcp1 antibody production, a peptide with the sequence SAPQ QPKQDSSQPAS, corresponding to amino acid residues 140–154 of dDcp1, was used to generate a polyclonal rabbit antiserum. For dDcp2 antibody production, the coding sequence of the dDcp2 C-terminal 289 amino acids (subcloned from EST clone SD14939) was cloned into the pRset vector for fusion protein expression and antibody generation. The detailed Western blot analysis, immunofluorescence staining, and coimmunoprecipitation protocols used are provided in the Supplemental Data.

In Situ Hybridization

The detailed protocol used is provided in the Supplemental Data.

Supplemental Data

Supplemental Data include a table, three figures, and Supplemental Experimental Procedures and are available at http://www.developmentalcell.com/cgi/content/full/10/5/601/DC1/.

Acknowledgments

We are indebted to all those who contributed to the construction of the *cFRT^{2L2R}* chromosome. We are grateful to Bob Boswell, Ira Clark, Ilan Davis, Anne Ephrussi, Peter Gergen, Tulle Hazelrigg, Thomas C. Kaufman, Kaijun Li, Akira Nakamura, Li-Mei Pai, Norbert Perrimon, Bill Saxton, Daniel St Johnston, Henry Sun, James E. Wilhelm, and the Bloomington Stock Center for their generous gifts of fly stocks and antibodies. We thank Megerditch Kiledjian, Michael B. Melnick, and Rich Binari for critical comments on the manuscript. We also thank the Confocal Microscope Lab, Instrumentation Center, NTU, for assistance with microscopy. This project is supported by grants from the National Sciences Council, the Frontier in Genome Medicine Program (NSC89-2318-B002-011-M51; NSC90-2318-B002-001-M51), and the Ministry of Education (89-B-FA01-1-4), Taiwan, Republic of China.

Received: October 29, 2005
Revised: February 4, 2006
Accepted: February 28, 2006
Published: May 8, 2006

References

Alphey, L., Jimenez, J., White-Cooper, H., Dawson, I., Nurse, P., and Glover, D.M. (1992). twine, a cdc25 homolog that functions in the male and female germline of *Drosophila*. Cell *69*, 977–988.

Andrei, M.A., Ingelfinger, D., Heintzmann, R., Achsel, T., Rivera-Pomar, R., and Luhrmann, R. (2005). A role for eIF4E and eIF4E-transporter in targeting mRNPs to mammalian processing bodies. RNA *11*, 717–727.

Ball, L.J., Jarchau, T., Oschkinat, H., and Walter, U. (2002). EVH1 domains: structure, function and interactions. FEBS Lett. *513*, 45–52.

Beelman, C.A., Stevens, A., Caponigro, G., LaGrandeur, T.E., Hatfield, L., Fortner, D.M., and Parker, R. (1996). An essential component of the decapping enzyme required for normal rates of mRNA turnover. Nature *382*, 642–646.

Berleth, T., Burri, M., Thoma, G., Bopp, D., Richstein, S., Frigerio, G., Noll, M., and Nusslein-Volhard, C. (1988). The role of localization of bicoid RNA in organizing the anterior pattern of the *Drosophila* embryo. EMBO J. *7*, 1749–1756.

Braat, A.K., Yan, N., Arn, E., Harrison, D., and Macdonald, P.M. (2004). Localization-dependent Oskar protein accumulation: control after the initiation of translation. Dev. Cell *7*, 125–131.

Brendza, R.P., Serbus, L.R., Duffy, J.B., and Saxton, W.M. (2000). A function for kinesin I in the posterior transport of oskar mRNA and Staufen protein. Science *289*, 2120–2122.

Brengues, M., Teixeira, D., and Parker, R. (2005). Movement of eukaryotic mRNAs between polysomes and cytoplasmic processing bodies. Science *310*, 486–489.

Castagnetti, S., and Ephrussi, A. (2003). Orb and a long poly(A) tail are required for efficient oskar translation at the posterior pole of the *Drosophila* oocyte. Development *130*, 835–843.

Chang, J.S., Tan, L., and Schedl, P. (1999). The *Drosophila* CPEB homolog, orb, is required for oskar protein expression in oocytes. Dev. Biol. *215*, 91–106.

Chou, T.B., and Perrimon, N. (1996). The autosomal FLP-DFS technique for generating germline mosaics in *Drosophila melanogaster*. Genetics *144*, 1673–1679.

Clark, I., Giniger, E., Ruohola-Baker, H., Jan, L.Y., and Jan, Y.N. (1994). Transient posterior localization of a kinesin fusion protein reflects anteroposterior polarity of the *Drosophila* oocyte. Curr. Biol. *4*, 289–300.

Coller, J., and Parker, R. (2005). General translational repression by activators of mRNA decapping. Cell *122*, 875–886.

Coller, J.M., Gray, N.K., and Wickens, M.P. (1998). mRNA stabilization by poly(A) binding protein is independent of poly(A) and requires translation. Genes Dev. *12*, 3226–3235.

Coller, J.M., Tucker, M., Sheth, U., Valencia-Sanchez, M.A., and Parker, R. (2001). The DEAD box helicase, Dhh1p, functions in mRNA decapping and interacts with both the decapping and deadenylase complexes. RNA *7*, 1717–1727.

Cougot, N., Babajko, S., and Seraphin, B. (2004). Cytoplasmic foci are sites of mRNA decay in human cells. J. Cell Biol. *165*, 31–40.

Edgar, B.A., and Datar, S.A. (1996). Zygotic degradation of two maternal Cdc25 mRNAs terminates *Drosophila*'s early cell cycle program. Genes Dev. *10*, 1966–1977.

Ephrussi, A., and Lehmann, R. (1992). Induction of germ cell formation by oskar. Nature *358*, 387–392.

Ephrussi, A., Dickinson, L.K., and Lehmann, R. (1991). Oskar organizes the germ plasm and directs localization of the posterior determinant nanos. Cell *66*, 37–50.

Ferraiuolo, M.A., Basak, S., Dostie, J., Murray, E.L., Schoenberg, D.R., and Sonenberg, N. (2005). A role for the eIF4E-binding protein 4E-T in P-body formation and mRNA decay. J. Cell Biol. *170*, 913–924.

Fillman, C., and Lykke-Andersen, J. (2005). RNA decapping inside and outside of processing bodies. Curr. Opin. Cell Biol. *17*, 326–331.

Gatfield, D., and Izaurralde, E. (2004). Nonsense-mediated messenger RNA decay is initiated by endonucleolytic cleavage in *Drosophila*. Nature *429*, 575–578.

Gonzalez-Reyes, A., Elliott, H., and St Johnston, D. (1995). Polarization of both major body axes in *Drosophila* by gurken-torpedo signalling. Nature *375*, 654–658.

Hachet, O., and Ephrussi, A. (2001). *Drosophila* Y14 shuttles to the posterior of the oocyte and is required for oskar mRNA transport. Curr. Biol. *11*, 1666–1674.

Khanna, R., and Kiledjian, M. (2004). Poly(A)-binding-protein-mediated regulation of hDcp2 decapping in vitro. EMBO J. *23*, 1968–1976.

Kim, Y.K., Furic, L., Desgroseillers, L., and Maquat, L.E. (2005). Mammalian Staufen1 recruits Upf1 to specific mRNA 3′UTRs so as to elicit mRNA decay. Cell *120*, 195–208.

Kim-Ha, J., Smith, J.L., and Macdonald, P.M. (1991). oskar mRNA is localized to the posterior pole of the *Drosophila* oocyte. Cell *66*, 23–35.

Li, K., and Kaufman, T.C. (1996). The homeotic target gene centrosomin encodes an essential centrosomal component. Cell *85*, 585–596.

Lykke-Andersen, J. (2002). Identification of a human decapping complex associated with hUpf proteins in nonsense-mediated decay. Mol. Cell. Biol. *22*, 8114–8121.

Mansfield, J.H., Wilhelm, J.E., and Hazelrigg, T. (2002). Ypsilon Schachtel, a *Drosophila* Y-box protein, acts antagonistically to Orb in the oskar mRNA localization and translation pathway. Development *129*, 197–209.

Micklem, D.R., Dasgupta, R., Elliott, H., Gergely, F., Davidson, C., Brand, A., Gonzalez-Reyes, A., and St Johnston, D. (1997). The mago nashi gene is required for the polarisation of the oocyte and the formation of perpendicular axes in *Drosophila*. Curr. Biol. *7*, 468–478.

Mohr, S.E., Dillon, S.T., and Boswell, R.E. (2001). The RNA-binding protein Tsunagi interacts with Mago Nashi to establish polarity and localize oskar mRNA during *Drosophila* oogenesis. Genes Dev. *15*, 2886–2899.

Nakamura, A., Amikura, R., Hanyu, K., and Kobayashi, S. (2001). Me31B silences translation of oocyte-localizing RNAs through the formation of cytoplasmic RNP complex during *Drosophila* oogenesis. Development *128*, 3233–3242.

Nakamura, A., Sato, K., and Hanyu-Nakamura, K. (2004). *Drosophila* cup is an eIF4E binding protein that associates with Bruno and regulates oskar mRNA translation in oogenesis. Dev. Cell *6*, 69–78.

Neuman-Silberberg, F.S., and Schupbach, T. (1993). The *Drosophila* dorsoventral patterning gene gurken produces a dorsally localized RNA and encodes a TGF α-like protein. Cell *75*, 165–174.

Newmark, P.A., and Boswell, R.E. (1994). The mago nashi locus encodes an essential product required for germ plasm assembly in *Drosophila*. Development *120*, 1303–1313.

Nilson, L.A., and Schupbach, T. (1999). EGF receptor signaling in *Drosophila* oogenesis. Curr. Top. Dev. Biol. *44*, 203–243.

Palacios, I.M., Gatfield, D., St Johnston, D., and Izaurralde, E. (2004). An eIF4AIII-containing complex required for mRNA localization and nonsense-mediated mRNA decay. Nature *427*, 753–757.

Parker, R., and Song, H. (2004). The enzymes and control of eukaryotic mRNA turnover. Nat. Struct. Mol. Biol. *11*, 121–127.

Ramirez, C.V., Vilela, C., Berthelot, K., and McCarthy, J.E. (2002). Modulation of eukaryotic mRNA stability via the cap-binding translation complex eIF4F. J. Mol. Biol. *318*, 951–962.

Ramos, A., Grunert, S., Adams, J., Micklem, D.R., Proctor, M.R., Freund, S., Bycroft, M., St Johnston, D., and Varani, G. (2000). RNA recognition by a Staufen double-stranded RNA-binding domain. EMBO J. *19*, 997–1009.

Rehwinkel, J., Behm-Ansmant, I., Gatfield, D., and Izaurralde, E. (2005). A crucial role for GW182 and the DCP1:DCP2 decapping complex in miRNA-mediated gene silencing. RNA *11*, 1640–1647.

Schwartz, D.C., and Parker, R. (2000). mRNA decapping in yeast requires dissociation of the cap binding protein, eukaryotic translation initiation factor 4E. Mol. Cell. Biol. *20*, 7933–7942.

Semotok, J.L., Cooperstock, R.L., Pinder, B.D., Vari, H.K., Lipshitz, H.D., and Smibert, C.A. (2005). Smaug recruits the CCR4/POP2/NOT deadenylase complex to trigger maternal transcript localization in the early *Drosophila* embryo. Curr. Biol. *15*, 284–294.

She, M., Decker, C.J., Sundramurthy, K., Liu, Y., Chen, N., Parker, R., and Song, H. (2004). Crystal structure of Dcp1p and its functional implications in mRNA decapping. Nat. Struct. Mol. Biol. *11*, 249–256.

Sheth, U., and Parker, R. (2003). Decapping and decay of messenger RNA occur in cytoplasmic processing bodies. Science *300*, 805–808.

Shulman, J.M., Benton, R., and St Johnston, D. (2000). The *Drosophila* homolog of *C. elegans* PAR-1 organizes the oocyte cytoskeleton and directs oskar mRNA localization to the posterior pole. Cell *101*, 377–388.

Steiger, M., Carr-Schmid, A., Schwartz, D.C., Kiledjian, M., and Parker, R. (2003). Analysis of recombinant yeast decapping enzyme. RNA *9*, 231–238.

St Johnston, D., Beuchle, D., and Nusslein-Volhard, C. (1991). Staufen, a gene required to localize maternal RNAs in the *Drosophila* egg. Cell *66*, 51–63.

Surdej, P., and Jacobs-Lorena, M. (1998). Developmental regulation of bicoid mRNA stability is mediated by the first 43 nucleotides of the 3′ untranslated region. Mol. Cell. Biol. *18*, 2892–2900.

Tharun, S., and Parker, R. (1999). Analysis of mutations in the yeast mRNA decapping enzyme. Genetics *151*, 1273–1285.

Theurkauf, W.E., and Hazelrigg, T.I. (1998). In vivo analyses of cytoplasmic transport and cytoskeletal organization during *Drosophila* oogenesis: characterization of a multi-step anterior localization pathway. Development *125*, 3655–3666.

Van Dijk, E., Cougot, N., Meyer, S., Babajko, S., Wahle, E., and Seraphin, B. (2002). Human Dcp2: a catalytically active mRNA decapping enzyme located in specific cytoplasmic structures. EMBO J. *21*, 6915–6924.

Van Doren, M., Williamson, A.L., and Lehmann, R. (1998). Regulation of zygotic gene expression in *Drosophila* primordial germ cells. Curr. Biol. *8*, 243–246.

van Eeden, F., and St Johnston, D. (1999). The polarisation of the anterior-posterior and dorsal-ventral axes during *Drosophila* oogenesis. Curr. Opin. Genet. Dev. *9*, 396–404.

van Eeden, F.J., Palacios, I.M., Petronczki, M., Weston, M.J., and St Johnston, D. (2001). Barentsz is essential for the posterior localization of oskar mRNA and colocalizes with it to the posterior pole. J. Cell Biol. *154*, 511–523.

Wang, Z., Jiao, X., Carr-Schmid, A., and Kiledjian, M. (2002). The hDcp2 protein is a mammalian mRNA decapping enzyme. Proc. Natl. Acad. Sci. USA *99*, 12663–12668.

Wilhelm, J.E., and Smibert, C.A. (2005). Mechanisms of translational regulation in *Drosophila*. Biol. Cell. *97*, 235–252.

Wilhelm, J.E., Mansfield, J., Hom-Booher, N., Wang, S., Turck, C.W., Hazelrigg, T., and Vale, R.D. (2000). Isolation of a ribonucleoprotein complex involved in mRNA localization in *Drosophila* oocytes. J. Cell Biol. *148*, 427–440.

Wilhelm, J.E., Hilton, M., Amos, Q., and Henzel, W.J. (2003). Cup is an eIF4E binding protein required for both the translational repression of oskar and the recruitment of Barentsz. J. Cell Biol. *163*, 1197–1204.

Wilsch-Brauninger, M., Schwarz, H., and Nusslein-Volhard, C. (1997). A sponge-like structure involved in the association and transport of maternal products during *Drosophila* oogenesis. J. Cell Biol. *139*, 817–829.

Wilusz, C.J., Gao, M., Jones, C.L., Wilusz, J., and Peltz, S.W. (2001). Poly(A)-binding proteins regulate both mRNA deadenylation and decapping in yeast cytoplasmic extracts. RNA *7*, 1416–1424.